Title	Analysis of geosynthetic tubes inflated by liquid and consolidated soil(Main article)
Author(s)	Guo, Wei; Chu, Jian; Nie, Wen
Citation	Guo, W., Chu, J., & Nie, W. (2014). Analysis of geosynthetic tubes inflated by liquid and consolidated soil. Geotextiles and Geomembranes, 42(4), 277-283.
Date	2014
URL	http://hdl.handle.net/10220/20924
Rights	© 2014 Elsevier Ltd. This is the author created version of a work that has been peer reviewed and accepted for publication by Geotextiles and Geomembranes. It incorporates referee’s comments but changes resulting from the publishing process, such as copyediting, structural formatting, may not be reflected in this document. The published version is available at: [http://dx.doi.org/10.1016/j.geotexmem.2014.05.001].

Analysis of Geosynthetic Tubes Inflated by Liquid and Consolidated Soil

Wei Guo[1*], Jian Chu[2] and Wen Nie[1]

[1]School of Civil and Environmental Engineering, Nanyang Technological University, Blk N1, 50 Nanyang Ave, Singapore, 639798
[2]Department of Civil, Construction & Environmental Engineering, Iowa State University, 328 Town Engineering Building, Ames, IA, 50011, USA, Email: jchu@iastate.edu
[*]Corresponding author, Tel.: 65-6592 3074; Fax: 65 67906620, E-mail: GuoWei@ntu.edu.sg

Abstract

When permeable geosynthetic tubes are used for dewatering of waste sludge or construction of dikes or embankments, the tubes have to be inflated using sludge or soil slurry several times. After each inflation, the soil slurry is consolidated into solid. Hence from the second inflation onwards, the geosynthetic tube is filled by both slurry and consolidated soil. In this paper, a new analytical method is proposed to provide a solution to the above specific case. Friction between geosynthetic sheet and soil, and friction between geosynthetic tube and subgrade, are considered. Parametric studies are also carried out to compare the design between geosynthetic tubes inflated using pure slurry and that using slurry and consolidated soil to study the key factors affecting the design. The study shows that tensile forces vary along the cross-section of the geosynthetic tube with the minimum value occurring at the center of the base. The effect of friction and lateral earth pressure on the geometry and tensile forces of the geosynthetic tube is insignificant when the height of the consolidated soil in the tube is small, but increases considerably with an increase in the height.

Keywords: Geotextile Tube; Geosynthetic Tube; Consolidated Soil.

1 Introduction

Geosynthetic tubes have been widely used in breakwaters and beach restoration projects in recent years (Leshchinsky et al., 1996; Shin and Oh, 2007; Lawson, 2008; Cantré and Saathoff, 2011; Yan and Chu, 2010; Chu et al., 2012; Yee et al., 2012; Yee and Lawson, 2012; Lee and Douglas, 2012). These tubes are made of geosynthetic materials and inflated with water, clay slurry or sand. Compared with traditional ways of constructing shoreline structures using rock or precast concrete units, the use of geosynthetic tubes offers several advantages. First, it is cost-effective. The use of a layer of geosynthetic sheet with soil to form a tube is often more economical than the use of concrete or rocks. Second, the construction process can be made simpler and faster. Third, local soils can be used as filling materials. If sand is not readily available, silty clay or clay slurry can be used as well (Yan and Chu, 2010; Chu et al., 2012; Yee et al., 2012; Yee and Lawson, 2012). Geosynthetic tubes are also used to dewater waste sludge such as digested bio-solids, sewage sludge, dredged materials (Moo-Young and Tucker, 2002), industrial solid wastes (Worley et al., 2008), fly ash (Muthukumaran and Ilamparuthi, 2006) and coal slurry.

When permeable geosynthetics are used to form geosynthetic tubes, the geosynthetic sheet will act as a filtering medium. The sand or clay slurry is firstly pumped into the geosynthetic tube as shown in Figure 1(a). Then under the self-weight of the fill material and the confining stress provided by the geosynthetic sheet, water seeps through the permeable geosynthetic sheet and the solids are kept inside the tube, see Figure 1(b). The total volume of the filling material inside the geosynthetic tube reduces considerably. To increase the volume of the solids inside the tube, the geosynthetic tube has to be refilled several times. From the second round of filling onwards as shown in Figure 1(c), the fill materials inside the tube become two parts: the newly pumped slurry and the consolidated soil left from the first pumping.

The analysis of geosynthetic tubes inflated by both slurry and consolidated soil is normally carried out using solutions for the analysis of geosynthetic tubes inflated with liquid or slurry. This is because most of the theoretical solutions available are for this type (Leshchinsky et al., 1996; Plaut and Suherman, 1998; Cantré and Saathoff, 2011; Yan and Chu, 2010; Chu et al., 2011; Guo et al, 2011; Malik and Sysala, 2011), except one solution provided by Plaut and Stephens (2012). However, the consolidated soils in the Plaut and Stephens's (2012) solution are still simulated as a liquid with a different density and a unit earth pressure coefficient at rest which may not be suitable for the case when the water content of the consolidated soils is relatively low.

In this paper, a new analytical method is proposed to analyze the permeable geosynthetic tubes inflated by slurry and consolidated soil at the time when the tube is just fully inflated. At this state (see Figure 1(c)), the fill materials in the geosynthetic tube consist of newly inflated slurry and the consolidated soil left from the previous step. The actions from the consolidated soils onto the geosynthetic tube are separated into effective earth pressure and pores water pressure. The properties of water in pore are the same as liquid. The force components from the effective earth pressure of the consolidated soil are separated along the lateral and vertical directions. The effects of the two force components to the geosynthetic tube depend on their relative force directions on the selected infinitesimal calculation element. The friction between the geosynthetic sheet and the fill materials and that between geosynthetic tube and subgrade are also considered in the method. A computer program was developed to solve the differential equations. The solution is applicable to analyze the permeable geosynthetic tube when it is just fully inflated by the new pumped slurry and consolidated soil left from the previous pumping.

2 **Derivation**

2.1 Basic assumptions

In deriving the solutions, the following assumptions need to be made: 1) the geosynthetic tube is sufficiently long to be assumed as a plane strain problem; 2) the geosynthetic shell is thin and its weight can be neglected; 3) the extension of the geosynthetic sheet is negligible; 4) the friction between geosynthetic and consolidated soil or that between geosynthetic and subgrade is sliding friction; 5) the top of the consolidated soil is horizontal; and 6) the water content or unit weight of the consolidated soil are constant during filling. Some of the above hypotheses are also made in the existing solutions for slurry inflated geosynthetic tubes (Szyszkowski and Glockner, 1987; Kazimierowicz, 1994; Plaut and Suherman, 1998; Cantré, 2002; Ghavanloo and Daneshmand, 2009; Cantré and Saathoff, 2011; Malik and Sysala, 2011; Chu et al, 2011; Guo et al, 2011; Plaut and Stephens, 2012; Guo et al., 2013).

2.2 Theoretical Derivations

A simplified cross-section of a geosynthetic tube inflated by new slurry and consolidated soil is shown in Figure 2(a). The coordinates system is set-up with x in the horizontal direction and y in the vertical direction. The origin of this coordinate is taken as the center of the contact edge with the rigid subgrade. The unit weight of the slurry is written as γ_L. The effective unit weight of the consolidated soil is denoted as γ_s' and $\gamma_s' = \gamma_s - \gamma_w$, where γ_s and γ_w are the unit weight of consolidated soil and water, respectively. The height of the consolidated soil is denoted as H_s. The height and width of the cross-section of the geosynthetic tube are written as H and B, respectively. The contact width between the tube and the subgrade is b. An infinitesimal small curve with a length of ds around an arbitrary point $S(x, y)$ can be treated as an arc with the center at point C and radius of r as shown in

Figure 2(b). The angle between the tangential direction at point $S(x, y)$ and the x axis is denoted as θ. Then two geometrical equations relating the angle between the tangential direction along cross section and the x and y coordinates can be written as Equations (1) and (2). For $x < b/2$, the contact part with the rigid subgrade is a straight line. Therefore, the calculation for the curvature is starting from $x = b/2$.

$$\frac{dy}{ds} = \sin\theta \tag{1}$$

$$\frac{dx}{ds} = \cos\theta \tag{2}$$

For the points below the surface of consolidated soils such as point $S(x, y)$ in Figure 2(a), two cases have to be considered separately based on the different position of point $S(x, y)$. The first case is when the angle between the tangent line on point $S(x, y)$ and the x-axis, θ, is less than $\pi/2$ as shown in Figure 2(a). The vertical effective earth pressure from the solid layer above point $S(x, y)$ is acting on it. The range of action could be mathematically expressed as $y < y_{slice} < y_D$ and $x\text{-}dx/2 < x_{slice} < x+dx/2$ where y_D is the calculation variable which is equal to the minimum value of H_s and the y-coordinate of the point that has the same x-coordinate with $S(x, y)$. The second case is when the angle between the tangent line on point $S(x, y)$ and the x-axis, θ, is greater than $\pi/2$, where the effective stress is not acting on it. In order to combine the two cases together, the total force from the vertical earth pressure acting internally on point $S(x, y)$ can be mathematically written as $\alpha\gamma_s'(y_D\text{-}y)\cos\theta\, ds$, where $\alpha = 1$ when $\theta < \pi/2$ and $\alpha = 0$ when $\theta > \pi/2$. Then the components due to the vertical effective earth pressure acting at point $S(x, y)$ in the normal and tangential directions are expressed as $\alpha\gamma_s'(y_D\text{-}y)\cos^2\theta ds$ and $\alpha\gamma_s'(y_D\text{-}y)\cos\theta\sin\theta ds$, respectively. The total force due to the lateral effective earth pressure can be calculated as $k\gamma_s'(H_s\text{-}y)\sin\theta ds$ where k is the coefficient of lateral earth pressure. The force components due to the lateral earth pressure that act on the point $S(x, y)$ in normal and tangential direction can be calculated as $k\gamma_s'(H_s-y)\sin^2\theta ds$ and $k\gamma_s'(H_s-y)sin\theta\cos\theta ds$, respectively. The friction, f, between filling solid layer and the geosynthetic sheet is calculated by multiplying the net resultant force in the normal direction, N, with the friction coefficient between solid filling material and geosynthetic sheet, μ_1, i.e. $f = \mu_1 N$ and $N = (k\gamma_s'(H_s-y)\sin^2\theta + \gamma_s'(y_D-y)\cos^2\theta)ds$. The direction of the friction force is the same as the direction indicated in Figure 2(a) because the whole tube is inflated to a sausage shaped cross-section and the solids are pulled up. It should be pointed out that there is no contact friction if there is no relative movement between the subgrade and the geosynthetic tube skin because the geotextile sheet is assumed to be inelastic. The method of using the friction coefficient multiplied by the normal stress acting on the point is a simplified approach. In the real case, it is possible to have relative movement between the geosynthetic tube and subgrade because of the extension of the geosynthetic material. The total force due to the hydraulic pressure acting at point $S(x, y)$ is written as $(p_0+\gamma_L(H-H_s)+\gamma_w(H_s-y))ds$ where p_0 is the pumping pressure on top of the geosynthetic tube. The tensile force along the cross-section is denoted as T. The tensile force additional along the differential direction is written as dT. Based on the free-body diagram of the infinitesimal element shown in Figure 2(b), equilibriums of the forces along the normal and tangential directions yields the following equations:

$$\frac{dT}{ds} = (\alpha(y_D - y) - k(H_s - y))\gamma_s^{'} \sin\theta\cos\theta + \mu_1 N \tag{3}$$

$$\frac{d\theta}{ds} = \frac{1}{T}[N + p_0 + \gamma_L(H - H_s) + \gamma_w(H_s - y)] \tag{4}$$

where $$N = \gamma_s^{'}(k(H_s - y)\sin^2\theta + \alpha(y_D - y)\cos^2\theta)ds \tag{5}$$

For the point above the surface of consolidated soils such as point $S(x, y)$ in Figure 3(a), the calculation procedure is the same as that used for liquid inflated geosynthetic tubes. A free body diagram of the infinitesimal calculation element at point $S(x, y)$ is shown in Figure 3(b). The hydraulic pressure acting internally on the tube at a given depth is written as $p_0 + \gamma_L (H - y)$. The tension force along the cross-section is constant because the friction between filling slurry and geosynthetic tube can be neglected. Based on the force equilibrium equations in the normal and tangential directions along the infinitesimal element, the following equations can be obtained:

$$\frac{dT}{ds} = 0 \tag{6}$$

$$\frac{d\theta}{ds} = \frac{1}{T}(p_0 + \gamma_L (H - y)) \tag{7}$$

2.3 Boundary Conditions

In order to solve the differential equations, one more boundary condition related to the tensile force has to be established. A free body diagram of the half cross-section is presented in Figure 4 where T_{top} and T_{bottom} are denoted as the tensile forces on top (point M) and bottom middle point (point N), respectively. Because the cross-section is symmetric and the tensile forces are along its tangential directions, the direction of T_{top} and T_{bottom} must be horizontal as shown in Figure 4. The tensile force on the bottom, T_{Bottom}, has to be calculated from the tensile force on the point $(b/2, 0)$ by considering contact friction between the geosynthetic tube and the rigid subgrade. The decreasing rate of tensile force can be simplified as $dT/dx = - \mu_1\gamma_s' y_D - \mu_2 W/b$ where W is the total weight of the filling material. Thus $T_{Bottom} = T_{(b/2, 0)} + \int_{b/2}^{x}(\mu_1\gamma_s' y_D + \mu_2 W/b)dx$ where x ranges from $b/2$ to x_b and x_b is the x-coordinate along the rigid contact surface when $T_{Bottom} = 0$ (if $T_{Bottom} > 0$, $x_b = 0$). It should be pointed out that the magnitude of y_D is from the calculated cross-section which is also an unknown variable. It will be further discussed in section 2.4 that a searching method (complex method) will be adapted to search for the target variables. Then for each searching loop, the y_D value is calculated from the cross-section of the previous loop. As the complex searching method narrows the range of the possible variables, the y_D value will become closer and closer to the real value. For the selected free body diagram in Figure 4, the forces acting along the horizontal direction involve the hydraulic pressure, the friction between the geosynthetic sheet and the ground ($\int_{b/2}^{xb}(\mu_2 W/b)dx$), and the tensile force in the geosynthetic sheet. Therefore, force equilibrium in the horizontal direction between these forces yields:

$$T_{Top} + T_{Bottom} = p_0 H + \frac{1}{2}\gamma_L (H^2 - H_s^{\ 2}) + \frac{1}{2}(\gamma_w + k\gamma_s^{'})H_s^2 + \mu_2 \frac{W}{b}(x_b - \frac{b}{2}) \tag{8}$$

By combining Equations (1) to (8), the geometry and tensile force of the geosynthetic tube inflated by slurry and consolidated soil could be solved by a computer program. The unit weight of soil, γ_s, unit weight of liquid (or slurry), γ_L, unit weight of water, γ_w, the thickness of the solid layer, H_s, the coefficient of lateral earth pressure, k, and any two parameters from p_0, L, H, are taken as inputs. The following two boundary conditions are adopted for the curved section: 1) when $y = 0$, $x = b/2$ and $\theta = 0$; and 2) when $y = H$, $x = 0$ and $\theta = \pi$.

2.4 Iteration Method

As there is no closed-form solution for the tensile force or cross-section of the geosynthetic tube from these differential equations, a computer program has been written to obtain a numerical solution using the adaptive Runge-Kutta-Merson method (RKM4). Programs for the RKM4 method had already been developed by Press et al. (2007), Xu (1995), Christiansen (1970) and Lukehart (1963). A mathematical programming scheme, the

Complex Method proposed by Box (1965), was used to search for the unknown parameters in a specific range. Details of the calculation procedure are given in Lipson (1977) and Xu (1995).

3 Parametric Studies

To better understand the influence of some major factors, parametric studies were carried out. The input variables are the circumference of the cross-section (L) and pumping pressure (p_0). The height of solid in the tube (H_s), the unit weight of consolidated soil (γ_s), unit weight of the filling slurry (γ_L), the friction coefficient (μ) and the coefficient of lateral earth pressure (k) are also taken as inputs. In order to avoid the influence of units, dimensionless parameters were used in the analysis whenever possible. The normalization method adopted in this paper was similar to that used by Plaut and Stephens (2012). The unit weights γ_L and γ_s were divided by γ_w; geometry parameters H_s, H, B and b were divided by L; the area of the cross-section was divided by L^2; pumping pressure was divided by $\gamma_w L$; and tensile force was divided by $\gamma_w L^2$. In the calculation, the unit weight of the fill slurry was taken as 1.2 times that of water, and the unit weight of the consolidated soil was 1.78 times that of water. The water content of the soil was taken as 40% and its specific gravity was 2.61.

Some comparisons of analytical results between geosynthetic tubes fully inflated by liquid and those inflated by liquid and consolidated soils are shown in Figure 5. Six different cases were considered to illustrate the effects of normalized height of consolidated soil, coefficient of lateral earth pressure and the friction coefficient. It should be noted that the lateral earth pressure may vary from an active case to a positive case depending on the reaction between geosynthetic tube and consolidated soil. It can be seen that the height of the geosynthetic tube inflated using liquid and consolidated soils is lower than that using liquid only. This is because of the influence from the soil heights and coefficient of lateral earth pressure. The difference is up to 18.4% for the case with $p_0/\gamma_w L$ = 0.3, H_s/L =0.2, k= 3.0 and μ = 0.5 as shown in Figure 5(b). Therefore, design for geosynthetic tubes inflated using liquid and consolidated soils using an analytical method for those using liquid alone will overestimate the height of the geosynthetic tube.

As shown in Figure 5, the tensile force distribution along the cross-section of a geosynthetic tube above the ground surface is uniform for a tube inflated with slurry alone. On the other hand, the tensile force distribution varies along a tube inflated using both slurry and consolidated soil with the maximum value occurring at the top of the tube, point D, and the minimum value at point A which is the center point at the base. The tensile force increases when the point moves from point A towards the boundary of the contact between the tube and the ground at B (Figure 5). The change in the tensile forces from A to B is due to the friction between the geosynthetic and the ground. For the tensile forces in section BC of the geosynthetic tube that does not contact with the ground, the tensile force distributions are also not uniform. Generally, the tensile force increases from point B towards C as shown in Figure 5 except for the case in Figure 5(b) because of the larger coefficient of lateral earth pressure (k = 3.0). Since the center point A has the smallest tensile force, it will be an ideal position to put the joint of the geosynthetic tube as the seam strength is usually lower than the geosynthetic itself (Gughelmetti et al. 1996; TenCate™, 2010; Guo 2012).

The relationships between the normalized pumping pressure and the normalized height of the geosynthetic tube are plotted in Figure 6 for different fills and friction conditions. The height of the tube is affected by the height of the consolidated soils, among other factors. The higher the height of the normalized consolidated soils, H_s/L, the lower the normalized height of the geosynthetic tube for a given normalized pumping pressure, $p_0/\gamma_w L$. The highest normalized height of the cross-section, H/L, occurs when the tube is filled by liquid only. This is consistent with the observation made in Figure 5. When H_s/L = 0.0, i.e. no solids are in the tube, the friction components have no influence on the height of the cross-section. This is because the friction is transmitted through the solids. When the height of the consolidated soils increases, the effect of the coefficient of lateral earth pressure becomes significant. Take the case when $H_s/L = 0.2$, $p_0/\gamma_w L = 0.02$, $\mu = 0.5$ in Figure 6, for example: H/L decreases by 22.3% from 0.148 to 0.115 when k varies from 0.65 to 3.0. Figure 7 shows the relationship between the pumping pressure and the normalized area of the cross-section, A/L^2, for different p_0, μ, k and H_s/L values. It is shown again that the normalized area of the cross-section will reduce when the height of the consolidated soils increases.

Figure 8 depicts the effect of $p_0/\gamma_w L$, μ, k and H_s/L on the relationships between the normalized width of the cross-section, B/L, and the normalized pumping pressure, $p_0/\gamma_w L$. It can be seen that B/L decreases with increasing $p_0/\gamma_w L$. The value of B/L is the smallest when the fill is only slurry. With the increase in the height of the consolidated soils, B/L increases to 0.39 for $H_s/L = 0.2$, $k = 3.0$, $\mu = 0.5$ and $p_0/\gamma_w L = 0.3$ or an increase of 10% compared with the case $H_s/L = 0$. This amount of difference needs to be considered when both slurry and consolidated soils are used to fill geosynthetic tubes. The effects of $p_0/\gamma_w L$, μ, k and H_s/L on the relationship between the normalized contact width with the ground, b/L, and the normalized pumping pressure, $p_0/\gamma_w L$, are shown in Figure 9. Similar observations as for B/L presented in Figure 8 can be made.

The normalized pumping pressure versus the normalized maximum tensile force $T_{max}/\gamma_w L^2$ is plotted in Figure 10 for different fill and friction conditions. It can be seen that the relationship is also unique. In other words, the $T_{max}/\gamma_w L^2$ value is only affected by the normalized pumping pressure and is not affected by whether the tube is filled with liquid or liquid and consolidated soil. Therefore, the maximum tensile force along the tube can be calculated using the theory of a geosynthetic tube inflated by slurry only. As mentioned before, the normalized minimum pumping pressure, $T_{min}/\gamma_w L^2$, is also affected by the fill and friction conditions as shown in Figure 11. For comparison, a curve for $T_{max}/\gamma_w L^2$ as shown in Figure 10 is also plotted in Figure 11. It can be seen that the maximum difference between the maximum and minimum tensile forces is $0.048\gamma_w L^2$ or 27.7% of $T_{max}/\gamma_w L^2$. However, this difference may not be considered in the design as the geosynthetic tube has to be inflated by slurry alone at least for the first time. The tensile strength of the geosynthetic sheet is still controlled only by the pumping pressure.

4 Conclusions

A new analytical solution was derived in this paper to analyze geosynthetic tubes inflated by slurry and consolidated soils left from previous pumping. Parametric studies were also carried out to evaluate the major factors affecting the tensile stresses and geometries of the tubes and the differences in the design for geosynthetic tubes inflated by slurry only and those by slurry and consolidated soils.

For geosynthetic tubes inflated by both slurry and consolidated soils, the tensile forces along the cross-section are not constant but have the maximum value occurring at the top of the tube and the minimum value at the center of the base section in contact with the subgrade. For geosynthetic tubes inflated with slurry alone, the tensile force along the cross-section above the ground surface is uniform and the value is about the same as the maximum tensile force in the geosynthetic tubes inflated with both slurry and consolidated soils. The maximum difference between the maximum and minimum values of tensile force is about 27.7%. As a geosynthetic tube has to be inflated with slurry alone when the tube is inflated for the first time, the tensile force calculation can be made using the solution for slurry filled geosynthetic tubes irrespective of the types of fill used. On the other hand, if the solution for liquid filled geosynthetic tubes is used for those filled with liquid and consolidated soils, the height of the geosynthetic tube will be overestimated by up to 18.4%, but the width underestimated by up to 10%. For these cases, the solution for geosynthetic tubes filled with slurry and consolidated soil should be used.

5 Notations

A	Area of cross-section
b	Contact width with subgrade
B	Width of cross-section
H	Height of cross-section
H_s	Height of the consolidated soil
k	Coefficient of lateral earth pressure
L	Perimeter of cross-section
p_0	Pumping pressure
r	Radius of the infinitesimal element
T	Tensile force along the geosynthetic tube per unit length
T_{max}	Maximum tensile force along the cross-section
T_{min}	Minimum tensile force along the cross-section
W	Total weight of the filling material
μ_1	Friction coefficient between consolidated soil and tube
μ_2	Friction coefficient between tube and subgrade
α	Non-dimensional parameter with its value of 0 or 1
γ'_s	Effective unit weight of consolidated soil
γ_L	Unit weight of filling slurry
γ_s	Unit weight of consolidated soil
γ_w	Unit weight of water
θ	The angle between *x* axis and the tangential direction at a point

6 References

Box, M.J., 1965. A new method of constrained optimization and comparison with other methods. Computer Journal 8 (1), 42-52.

Cantré, S., 2002. Geotextile tubes--analytical design aspects. Geotextiles and Geomembranes 20 (5), 305-319.

Cantré, S., Saathoff, F., 2011. Design method for geotextile tubes considering strain - Formulation and verification by laboratory tests using photogrammetry. Geotextiles and Geomembranes 29 (3), 201-210.

Christiansen, J., 1970. Numerical solution of ordinary simultaneous differential equations of the 1st order using a method for automatic step change. Numerische Mathematik 14 (4), 317-324.

Chu, J., Guo, W., Yan, S.W., 2011. Geosynthetic tubes and geosynthetic mats: analyses and applications. Geotechnical Engineering 42 (1), 56-65.

Chu, J., Yan, S. W., Li, W., 2012. Innovative methods for dike construction– An overview. Geotextiles and Geomembranes 30, 35-42.

Ghavanloo, E., Daneshmand, F., 2009. Two-dimensional analytical analysis of equilibrium shape of inflated geomembrane tube resting on rigid foundation with arbitrary shape. Geotextiles and Geomembranes, 27 (2), 99-106.

Gughelmetti, J.L., Koerner, G.R., Battino, F.S., 1996. Geotextile reinforcement of soft landfill process sludge to facilitate final closure: An instrumented case study. Geotextiles and Geomembranes 14 (7-8), 377-391.

Guo, W., Chu, J., Yan, S.W., 2011. Effect of subgrade soil stiffness on the design of geosynthetic tube. Geotextiles and Geomembranes 29 (3), 277-284.

Guo, W., 2012. Geosynthetic tubes and mats: experimental and analytical studies. PhD thesis, Nanyang Technological University, Singapore.

Guo, W., Chu, J., Yan, S.W., Nie, W., 2013. Geosynthetic mattress: Analytical solution and verification. Geotextiles and Geomembranes 37, 74-80.

Kazimierowicz, K., 1994. Simple analysis of deformation of sand-sausages. Fifth International Conference on Geotextiles, Geomembranes and Related Products, Hydraulic Applications and Related Research, Singapore 2, 775-778.

Lawson, C.R., 2008. Geotextile containment for hydraulic and environmental engineering. Geosynthetics International 15 (6), 384 – 427.

Lee, E.C., Douglas, R.S., 2012. Geotextile tubes as submerged dykes for shoreline management in Malaysia. Geotextiles and Geomembranes 30, 8-15.

Leshchinsky, D., Leshchinsky, O., Ling, H.I., Gilbert, P.A., 1996. Geosynthetic tubes for confining pressurized slurry: some design aspects. Journal of Geotechnical Engineering 122 (8), 682-690.

Lipson, S.L., Gwin, L.B., 1977. The complex method applied to optimal truss configuration. Computers & Structures 7 (3), 461-468.

Lukehart, P.M., 1963. Algorithm 218. Kutta Merson. Comm. Assoc. Comput. Mach. 6, 737-738.

Malik, J., Sysala, S., 2011. Analysis of geosynthetic tubes filled with several liquids with different densities. Geotextiles and Geomembranes 29 (3), 249-256.

Moo-Young, H.K., Tucker, W.R., 2002. Evaluation of vacuum filtration testing for geotextile tubes. Geotextiles and Geomembranes 20 (3), 191-212.

Muthukumaran, A.E., Ilamparuthi, K., 2006. Laboratory studies on geotextile filters as used in geotextile tube dewatering. Geotextiles and Geomembranes 24 (4), 210-219.

Plaut, R., Suherman, S., 1998. Two-dimensional analysis of geosynthetic tubes. Acta Mechanica 129 (3-4), 207-218.

Plaut, R.H., Stephens, T.C., 2012. Analysis of geotextile tubes containing slurry and consolidated material with frictional interface. Geotextiles and Geomembranes 32, 38-43.

Press, W., Teukolsky, S., Vetterling, W., Flannery, B., 2007. Section 17.1 Runge-Kutta Method, Numerical Recipes: The Art of Scientific Computing 3rd ed. Cambridge University Press, New York.

Szyszkowski, W., Glockner, P.G., 1987. On the statics of large-scale cylindrical floating membrane containers. International Journal of Non-Linear Mechanics 22 (4), 275-282.

TenCate, 2010. Seaming of geosynthetics, TenCatTM Geosynthetics North America, Pendergrass, GA, http://www.tencate.com.

Worley, J.W., Bass, T.M., Vendrell, P.F., 2008. Use of geotextile tubes with chemical amendments to dewater dairy lagoon solids. Bioresource Technology 99 (10), 4451-4459.

Xu, S.L., 1995. C-algorithms commonly used procedures set (2nd edition). Tsinghua University Press, Beijing, China, (In Chinese).

Shin, E.C., Oh, Y.I., 2007. Coastal erosion prevention by geotextile tube technology. Geotextiles and Geomembranes, 25 (4-5): 264-277.

Yan, S.W., Chu, J., 2010. Construction of an offshore dike using slurry filled geotextile mats. Geotextiles and Geomembranes 28 (5), 422-432.

Yee, T.W., Lawson, C.R., Wang, Z.Y., Ding, L., and Liu, Y., 2012. Geotextile tube dewatering of contaminated sediments, Tianjin Eco-City, China. Geotextiles and Geomembranes 31, 39-50.

Yee T. W., Lawson C. R., 2012. Modelling the geotextile tube dewatering process. Geosynthetics International 19 (5), 339 –353.

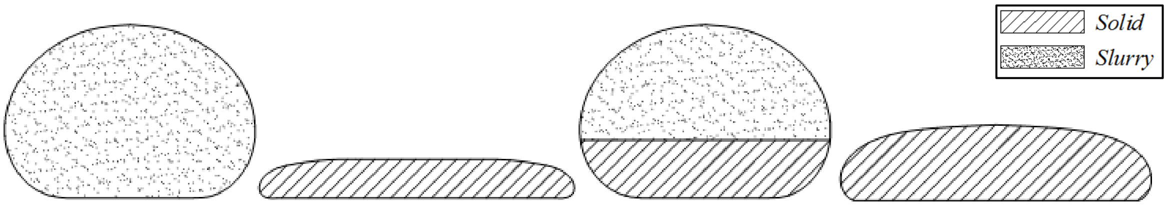

(a) 1st inflation (b) Dewatering after 1st inflation (c) 2nd inflation (d) Dewatering after 2nd inflation

Figure 1 Inflation process of the permeable geosynthetic tubes

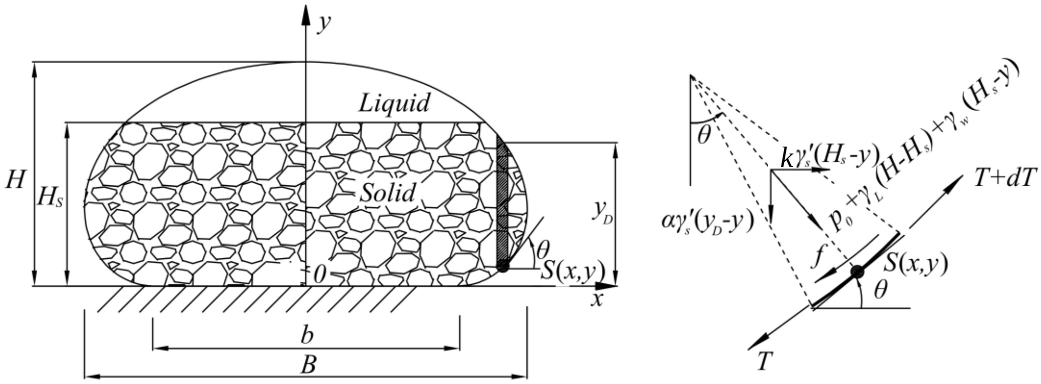

a) Cross-section of geosynthetic tube b) Free body diagram of infinitesimal element

Figure 2 Analytical model for geosynthetic tube inflated with liquid and consolidated soil when the infinitesimal element is below the surface of consolidated soils

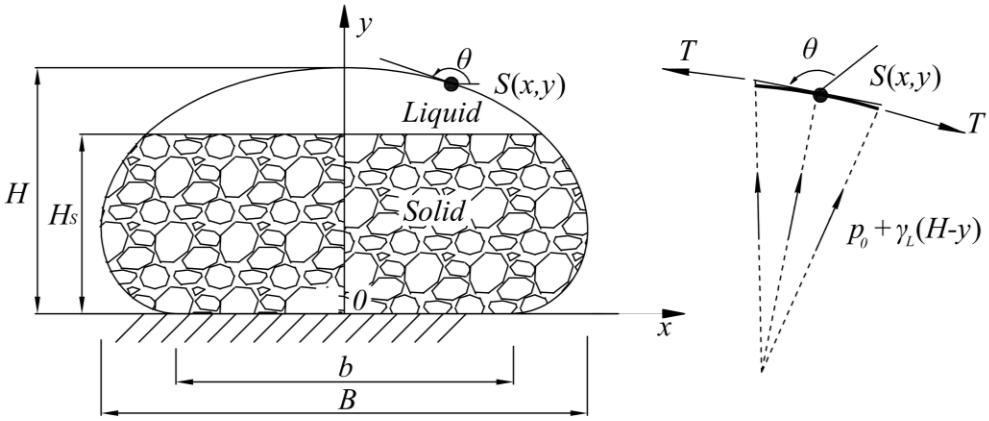

a) Cross-section of geosynthetic tube   b) Free body diagram of infinitesimal element

Figure 3 Force equilibrium analysis for geosynthetic tube when the infinitesimal element is above the surface of consolidated soils

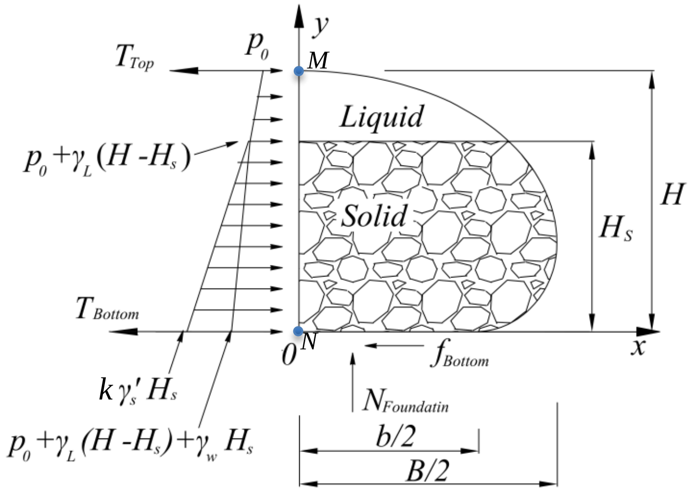

Figure 4 Force analysis for a cross-section along the vertical centerline

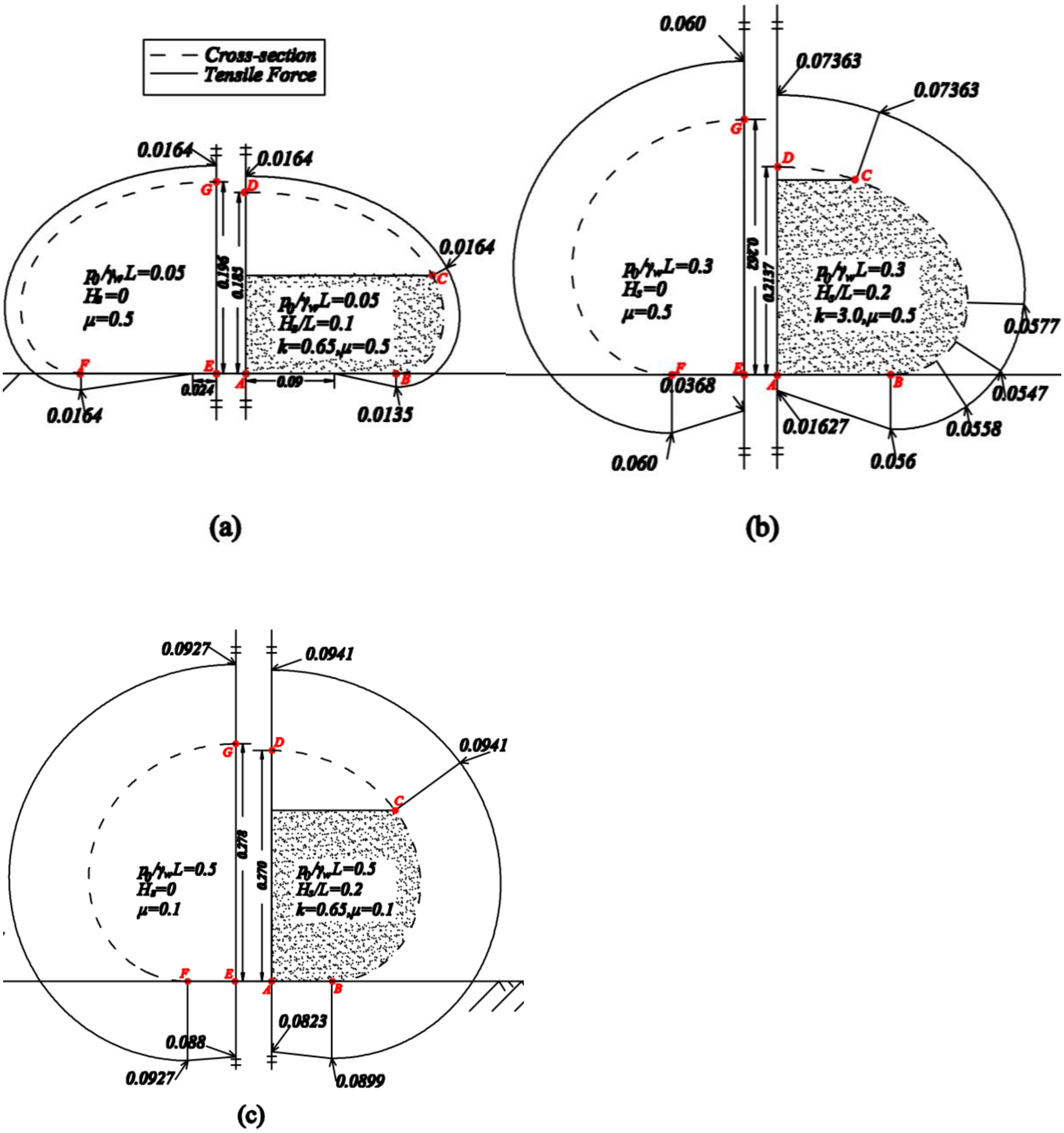

Figure 5 Comparisons of cross-section and tensile force of geosynthetic tube inflated by slurry (left-hand-side) and that by slurry and consolidated soils (right-hand-side) under different conditions: (a) $p_0/\gamma_w L$=0.05, H_s=0, μ=0.5 (*left*) and H_s/L=0.1, k=0.65 (*right*); (b) $p_0/\gamma_w L$=0.3, H_s=0, μ=0.5 (*left*) and H_s/L=0.2, k=3.0 (*right*); (c) $p_0/\gamma_w L$=0.5, H_s=0, μ=0.1 (*left*) and H_s/L=0.2, k=0.65 (*right*)

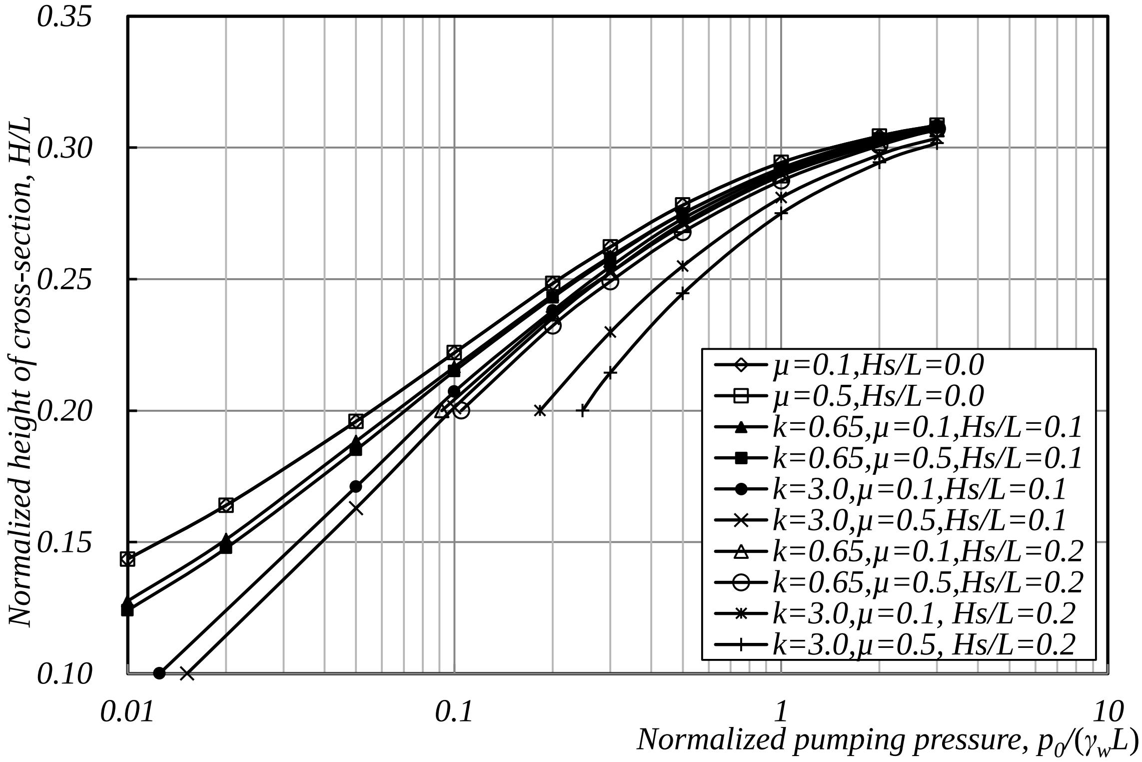

Figure 6 Normalized height of cross-section vs. normalized pumping pressure for different conditions

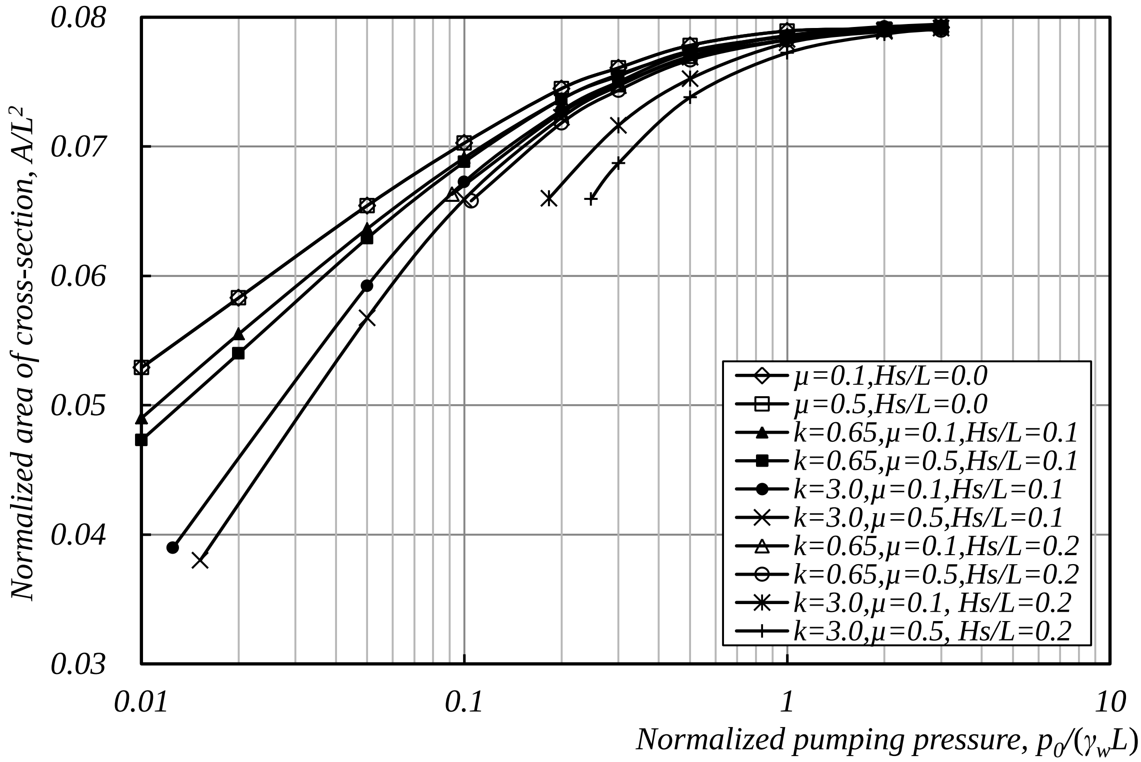

Figure 7 Characteristics of normalized area of cross-section vs. pumping pressure

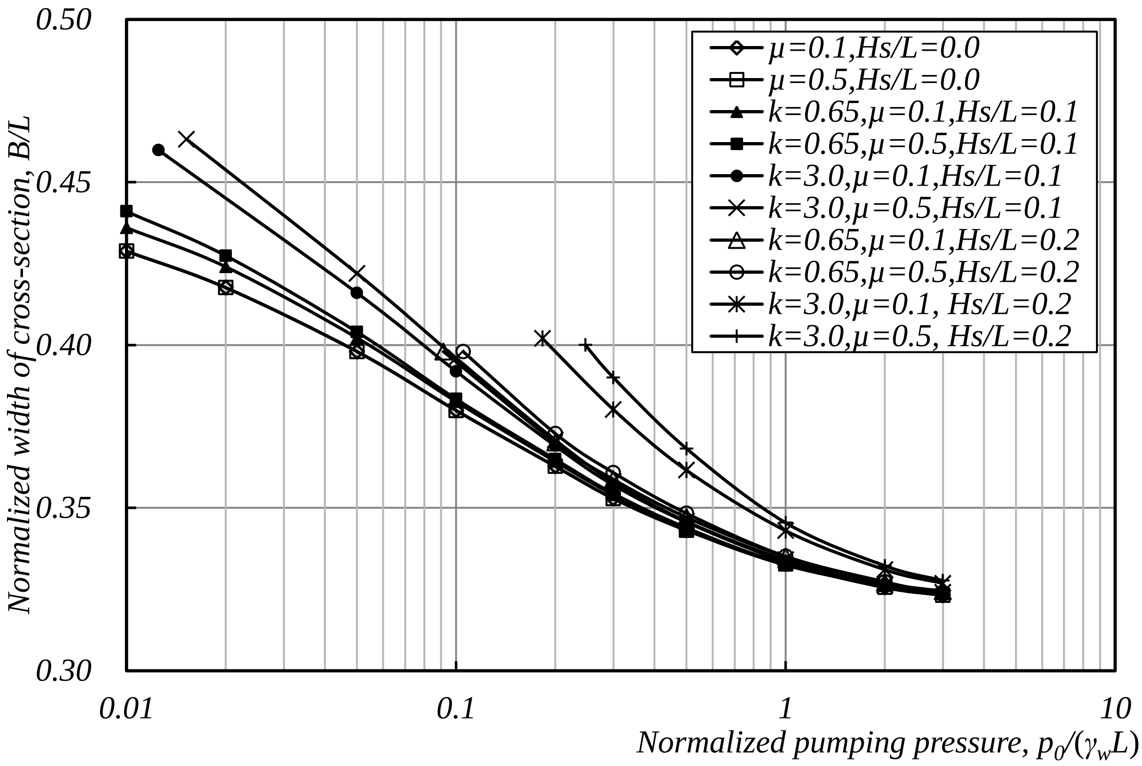

Figure 8 Characteristics of normalized width of cross-section vs. pumping pressure

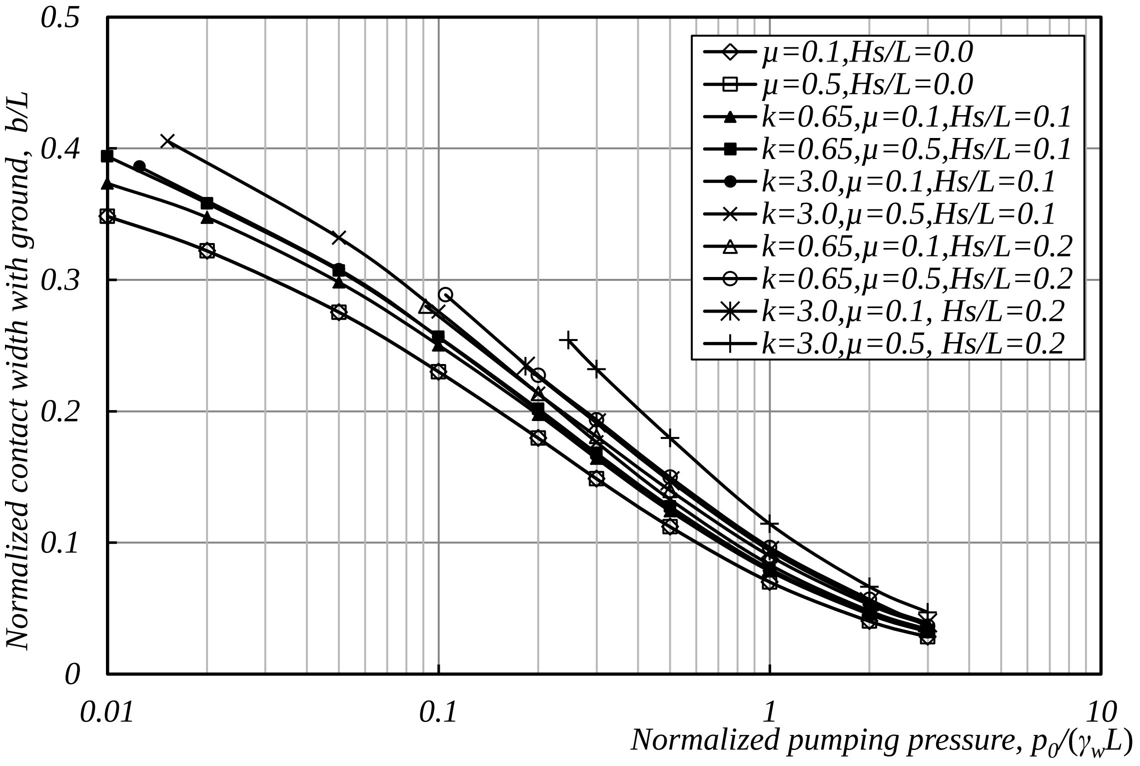

Figure 9 Characteristics of normalized contact width with ground vs. pumping pressure

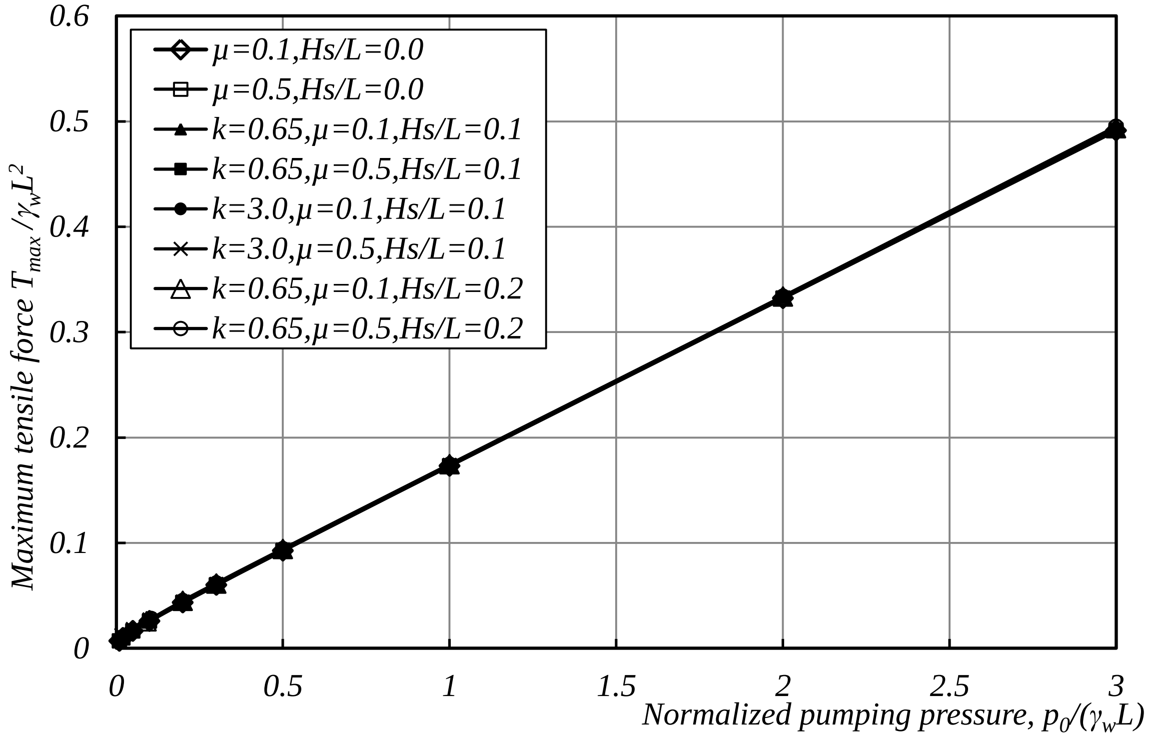

Figure 10 Characteristics of normalized T_{max} vs. pumping pressure

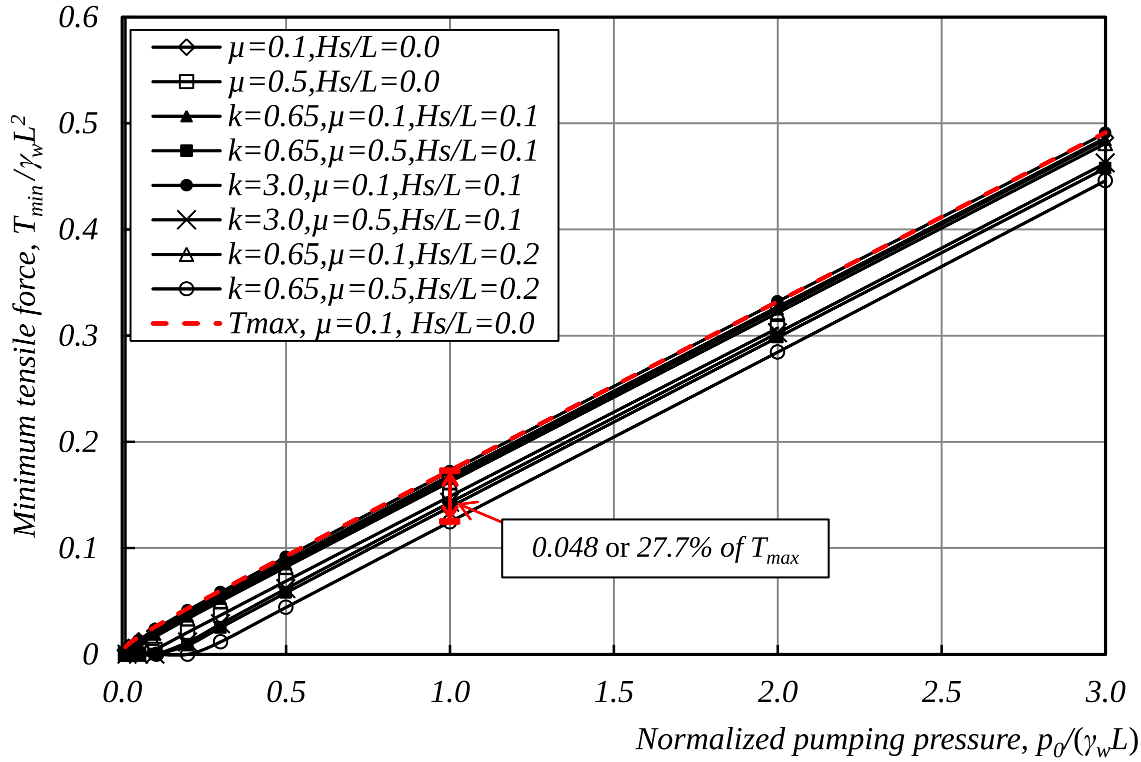

Figure 11 Characteristics of normalized T_{min} vs. pumping pressure